Astronomy & Astrophysics manuscript no. messina-astro-ph
December 21, 2009

RACE-OC Project: Rotation and variability in the open cluster M 11 (NGC 6705)⋆

S. Messina[1], P. Parihar[2], J.-R. Koo[3], S.-L. Kim[3], S.-C. Rey[4], and C.-U. Lee[3]

[1] INAF-Catania Astrophysical Observatory, via S. Sofia 78, I-95123 Catania, Italy
e-mail: sergio.messina@oact.inaf.it
[2] Indian Institute of Astrophysics, Block II, Koramangala, Bangalore India, 560034
e-mail: psp@iiap.res.in
[3] Korea Astronomy and Space Science Institute, Daejeon, Korea
e-mail: koojr@kasi.re.kr; slkim@kasi.re.kr
[4] Department of Astronomy and Space Science, Chungnam National University, Daejeon, Korea

ABSTRACT

Context. Rotation and magnetic activity are intimately linked in main-sequence stars of G or later spectral types. The presence and level of magnetic activity depend on stellar rotation, and rotation itself is strongly influenced by strength and topology of the magnetic fields. Open clusters represent especially useful targets to investigate the rotation/activity/age connection. Over the time stellar activity and rotation evolve, providing us with a promising diagnostic tool to determine age of the field stars.
Aims. The open cluster M11 has been studied as a part of the RACE-OC project (**R**otation and **AC**tivity **E**volution in **O**pen **C**lusters), which is aimed at exploring the evolution of rotation and magnetic activity in the late-type members of open clusters with different ages.
Methods. Photometric observations of the open cluster M11 were carried out in June 2004 using LOAO 1m telescope. The rotation periods of the cluster members are determined by Fourier analysis of photometric data time series. We further investigated the relations between the surface activity, characterized by the light curve amplitude, and rotation.
Results. We have discovered a total of 75 periodic variables in the M11 FoV, of which 38 are candidate cluster members. Specifically, among cluster members we discovered 6 early-type, 2 eclipsing binaries and 30 bona-fide single periodic late-type variables. Considering the rotation periods of 16 G-type members of the almost coeval 200-Myr M34 cluster, we could determine the rotation period distribution from a more numerous sample of 46 single G stars at an age of about 200-230 Myr and determine a median rotation period P=4.8d.
Conclusions. A comparison with the younger M35 cluster (∼150 Myr) and with the older M37 cluster (∼550 Myr) shows that G stars rotate slower than younger M35 stars and faster than older M37 stars. The measured variation of the median rotation period is consistent with the scenario of rotational braking of main-sequence spotted stars as they age. Finally, G-type M11 members have a level of photospheric magnetic activity, as measured by light curve amplitude, comparable to that observed in the in younger 110-Myr Pleiades stars of similar mass and rotation.

Key words. Stars: activity - Stars: late-type - Stars: rotation - Stars: starspots - Stars: open clusters and associations: individual: M11

1. Introduction

RACE-OC, which stands for **R**otation and **AC**tivity **E**volution in **O**pen **C**lusters, is a long-term project with the aim to study stellar rotation, magnetic activity, and their evolution in the late-type members of open clusters (Messina 2007; Messina et al. 2008a). The project's targets are open clusters which, differently than field stars, provide us with a sample of stars spanning a range of masses with same age, initial chemical composition, environmental conditions, and interstellar reddening. Such stellar samples allow us to accurately investigate the rotation/activity/age relashionships and their mass dependence.

Indeed, rotation is one basic property of late-type stars. It undergoes dramatic changes along the stellar life, as shown by observational studies and also predicted by evolution models of angular momentum (Kawaler 1988; MacGregor & Brenner 1991; Krishnamurthi et al. 1997; Bouvier et al. 1997; Sills et al. 2000; Ivanova & Taam 2003; Holzwarth & Jardine 2007). On one hand the properties of magnetic fields depend on rotation and mass, on the other hand, they play a fundamental role in altering the rotational properties of late-type stars. For example, they are responsible for the angular momentum loss and for the coupling mechanisms between the radiative core and the external convection zone (e.g., Barnes 2003). Such an interplay between rotation and magnetic fields provides us with a powerful tool to probe the stellar internal structure.

A number of valuable ongoing projects (MONITOR, Hodgkin et al. 2006; EXPLORE/OC, Extrasolar Planet Occultation Research, von Braun et al. 2005; RCT, Robotically Controlled Telescope project, Guinan et al.

Send offprint requests to: Sergio Messina

⋆ Figs. **??-??** are only available in electronic form at the CDS via anonymous ftp to cdsarc.u-strasbg.fr (130.79.128.5) or via http://cdsweb.u-strasbg.fr/cgi-bin/qcat?J/A+A/

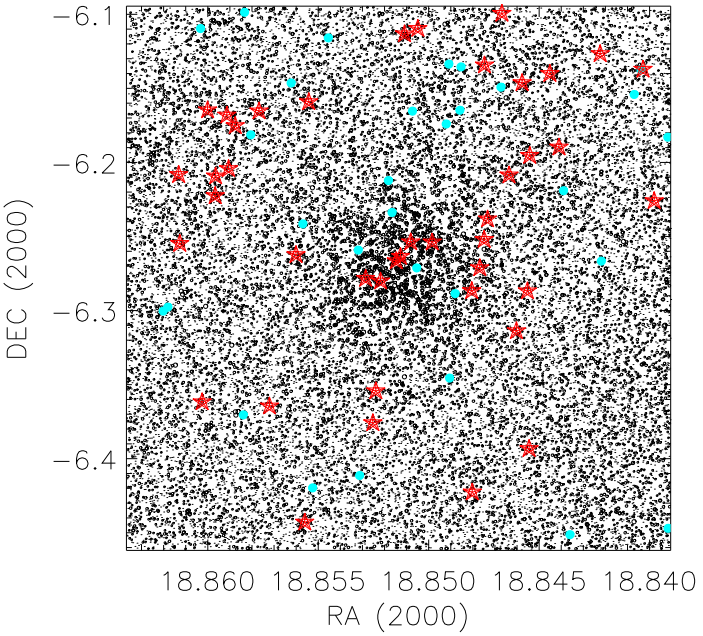

Fig. 1 M 11 field of view (22.2′× 22.2′). The newly discovered and previously known periodic variables are plotted as large red stars and light-blue bullets, respectively

2003) are rapidly increasing our knowledge of the rotational properties of late-type members of open clusters. However, the sequence of ages at which the angular momentum evolution has been studied still has significant gaps, and the sample of periodic cluster members is not as complete as necessary to fully constrain the various models proposed to describe the driving mechanisms of the angular momentum evolution.

We have selected open clusters (Messina 2007) and young associations (Messina el al. 2009) with an age in the range from 1 to 500 Myr and, generally, with no earlier rotation and magnetic activity studies. Top priority is given to the open clusters that fill the gaps in the empirical description of the rotation/activity/age relationships. We have selected also a few extensively studied clusters such as the Pleiades and the Orion Nebula Cluster (Parihar et al. 2009). The motivation is to make repeated observations over several years to further enrich the sample of periodic variables and to explore the long-term magnetic activity, e.g., to search for activity cycles and surface differential rotation (SDR). Our sample also includes open clusters that were previously monitored with different scientific motivations. The re-analysis of these archived data time series can provide valuable results in the context of the RACE-OC project. That was the case of M37 (Messina et al. 2008a, hereinafter Paper I). Although it was initially observed to search for early-type pulsating variables (Kang et al. 2007), its data time series allowed us to determine, for the first time, the rotation period distribution of G stars at an age of about 550 Myr. Similarly, the M11 photometric data time series which were collected with the same goal (Koo et al. 2007), have allowed us to determine, again for the first time, the rotation period distribution of G stars at an age of about 230 Myr.

M 11 (NGC 6705; $RA_{J2000.0}$ = 18:51:04, $DEC_{J2000.0}$ = −06:16:30) is a ∼230 Myr intermediate-age open cluster at a distance of nearly d=2.0 kpc, (m−M)=12.69±0.1. The cluster is subjected to substantial reddening E(B−V)=0.428 mag because of low galactic latitude (b=−2.8°). It contains thousands of members within an estimated radius of 16 arcmin. Gonzalez & Wallerstein (2000) found a small metal excess, +0.10 dex, in agreement with the general trend of increasing metallicity with decreasing distance from the Galactic center. In the following analysis we adopt the cluster parameters derived by Sung et al. (1999).

The first comprehensive variability study of M11 was carried out in 2002-2003 by Hargis et al. (2005) in the R band and on a 13.7′×13.7′ field of view. They discovered 39 variables, and for 32 of these they could determine the periodicity. Among late-type stars (B−V > 0.55), Hargis et al. (2005) could identify only 15 periodic eclipsing binaries, probably because of the large amplitude of light variation, but no periodic single stars. The poor seeing (∼ 5 arcsecond), the use of a small telescope and the faintness of the cluster late-type members at a distance of about 2kpc did not allow them to acquire sufficiently precise data required to detect very low amplitude variation due to spots. A second comprehensive variability study of M11 was carried out in 2004 by Koo et al. (2007), who detected all the variables previously found by Hargis et al. (2005) and 43 new periodic variables. Among late-type stars, they discovered 12 W UMa and 2 detached eclipsing binaries. Again, they did not report the discovery of any late-type low-amplitude periodic single stars, their study being focused on early-type pulsating variables.

Our investigation, which is based on the Koo et al. (2007) database, aims at detecting the periodicity of the low-amplitude late-type single members of M11. In Sect. 2 we give details on observations and data analysis. The rotation period search is presented in Sect. 3, the results in Sect. 4. Discussion and conclusions are given in Sect.5 and 6.

2. Observations and data analysis

The present study is based on observations taken in June 2004 with the 1.0m telescope at the Mt. Lemmon Optical Astronomy Observatory (LOAO) in Arizona (USA), which feeds a 2K×2K CCD camera. The observed field of view (FoV) is about 22.2′ × 22.2′ (see Fig. 1) at the f/7.5 Cassegrain focus. We collected a sequence of 406 long- (600 s) and 595 short-exposed (60 s) images in the V-band filter over a total time interval of 18 days. Additional observations in the B bandpass filter were made on one night of October 2004, in order to construct a V vs. B−V color-magnitude diagram. A detailed description of these observations and data reduction can be found in Koo et al. (2007) and Kim et al. (2001).

We detected about 33400 stars in the 12 < V < 20 magnitude range in the 600-s long exposures. Their coordinates, B and V magnitudes are available in the WEBDA open cluster database[1]. These stars are represented in Fig. 1 with open circles. The symbol size is proportional to the star's brightness. The over-plotted large red stars and light-blue bullets represent the newly discovered and already known

[1] http://www.univie.ac.at/webda/archive_ngc.html

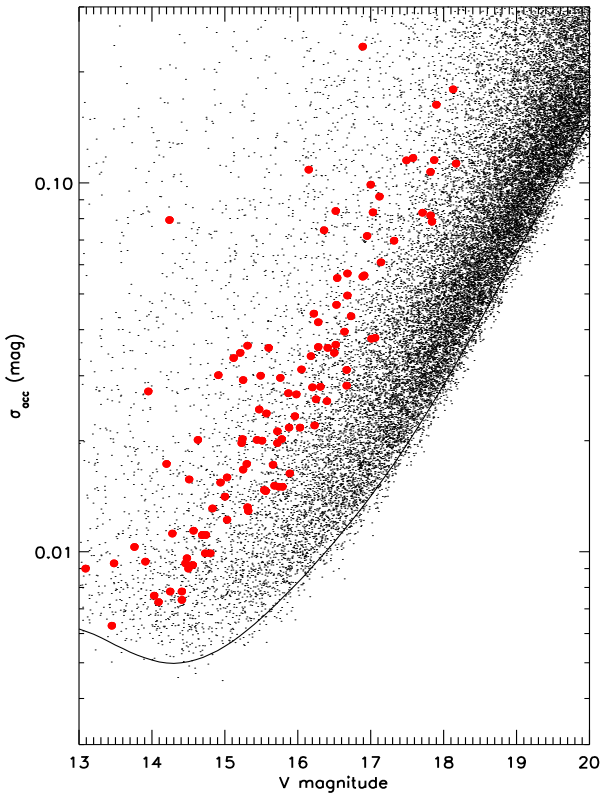

Fig. 2 Photometric accuracy $\sigma_{\rm acc}$ vs. mean magnitude for the stars in the M11 FoV. The solid line represents a polynomial fit to the distribution lower envelope. Small red bullets represent the periodic variable stars.

periodic variables in the FoV under analysis.

Before analysing our magnitude time series for the rotation period search, we took care to eliminate possible outliers. First we disregarded all data points that deviated more than 4 standard deviations from the mean of the whole series data. Such a broad limit was adopted to include the light minima of possible eclipsing binaries. In fact, we are aware from earlier studies of the presence of numerous eclipsing binaries in our FoV. Then, we computed a filtered version of the light curve by means of a sliding median boxcar filter with a boxcar extension equal to 1 hr. This filtered light curve was subtracted from the original light curve and all the points deviating more than 3 standard deviations of the residuals were discarded. Finally, we computed normal points by binning the data on time intervals having the duration of about 1 hr, getting a light curve consisting of about 100 normal points on average. Each normal point is obtained by averaging about 4 consecutive frames collected within a time interval of 1 hr. We adopted the average standard deviation of our normal points $\sigma_{\rm acc}$ as photometric accuracy of our observations, rather than the values computed by DAOPHOT while extracting the PSF magnitudes. This standard deviation $\sigma_{\rm acc}$ is an empirical estimate of the effective precision of our photometry. It represents a conservative value because the true observational accuracy could be, in principle, even better for stars showing substantial variability within the timescale closer to our fixed binning time interval. In Fig. 2 we plot $\sigma_{\rm acc}$ of the stars in the $13.0 < {\rm V} < 20.0$ magnitude range vs. their mean V magnitude. The lower envelope of the $\sigma_{\rm acc}$ distribution is populated by non variable and variable stars with least intrinsic variation. Such a lower envelope gives a measure of the best photometric accuracy we achieved at different magnitudes. In order to construct the relation between observational accuracy and magnitude, we fitted a multi-order polynomial function to the lower $\sigma_{\rm acc}$ boundary. The 600-s long exposures have allowed us to achieve a photometric accuracy $\sigma_{\rm acc}$ in the V band of about 0.006 mag in the $13 < {\rm V} < 16$ magnitude range, and better than 0.02 mag for all stars in the magnitude range $16.0 < {\rm V} < 18$.

We note that the photometric accuracy is slightly poorer than the accuracy we achieved for M37 (Paper I), although we have used the same telescope, instrumental setup, and reduction procedure. M 11 has a distance modulus about 1 magnitude larger than M37, is very rich, crowded and younger than M37. For example, our candidate periodic stars have on average 2 closeby stars within 5 arcsec and with a brightness difference down to 3 magnitudes. However, we adopted the PSF photometry which is the most accurate approach to determine the star's magnitude in crowded fields and which should eliminate any spurious flux contribution from closeby stars. Therefore, we suspect that the slightly poorer photometric accuracy of M11 with respect to M37 arises from its younger age and, specifically, from the higher level of short-scale (< 1hr) intrinsic variability.

3. Rotation period search

We have used the Scargle-Press method to search for significant periodicities related to the stellar rotation in our data time series. In the following sub-sections we briefly describe our procedures to identify the periodic variables. The period search was carried out on the 1-hr binned data time series, that is on about 100 data points with respect to the original series of about 400 frames, and after discarding evident outliers, as discussed in the previous section.

3.1. Scargle-Press periodogram

The Scargle technique has been developed in order to search for significant periodicities in unevenly sampled data (Scargle 1982; Horne & Baliunas 1986). The algorithm calculates the normalized power $\mathrm{P}_N(\omega)$ for a given angular frequency $\omega = 2\pi\nu$. The highest peaks in the calculated power spectrum (periodogram) correspond to the candidate periodicities in the analyzed data time series. In order to determine the significance level of any candidate periodic signal, the height of the corresponding power peak is related with a false alarm probability (FAP), that is the probability that a peak of given height is due to simply statistical variations, i.e. to Gaussian noise. This method assumes that each observed data point is independent from the others. However, this is not strictly true for our data time series consisting of data consecutively collected within the same night and with a time sampling much shorter than both the periodic or the irregular intrinsic variability timescales we

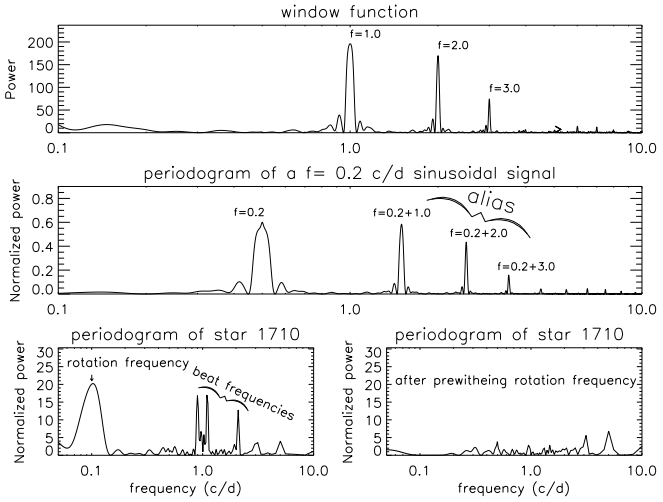

Fig. 3 *Top panel*: typical window function deriving from the data sampling and total time interval of the M11 observations. *Middle panel*: aliasing effect of the window function on an example periodic signal with frequency f=0.2 cd^{-1}. *Bottom left panel*: periodogram of star 1710 with rotation frequency together with its beat frequencies. *Bottom right panel*: disappearing of beat frequencies after prewhitening the rotation frequency.

are looking for (P^d=0.1-15). The impact of this correlation on the period determination has been highlighted by, e.g., Herbst & Wittenmyer (1996), Stassun et al. (1999), Rebull (2001), Lamm et al. (2004). In order to overcome this problem, we decided to determine the FAP in different way than proposed by Scargle (1982) and Horne & Baliunas (1986), the latter being only based on the number of independent frequencies.

3.2. False alarm probability

Following the approach outlined by Herbst et al. (2002), randomized time series data sets were created by randomly scrambling the day number of the Julian day while keeping photometric magnitudes and the decimal part of the JD unchanged. This method preserves any correlation that exists in the original data set. We noticed that Lamm et al. (2004) in order to produce the simulated light curves, randomized the observed magnitudes, instead of the epochs of observation. Then, we applied the periodogram analysis to about 10,000 "randomized" data time series for each star. We retained the highest power peak and the corresponding period of each computed periodogram. The FAP related to a given power P_N is taken as the fraction of randomised light curves that have the highest power peak exceeding P_N which, in turn, is the probability that a peak of this height is simply due to statistical variations, i.e. white noise. The normalised power corresponding to a FAP = 0.01 was found to be P_N= 9.2.

3.3. Alias detection

In order to identify the true periodicities in the periodogram, it is crucial to take into account that a few peaks, even with large power, are aliases arising from both the data sampling and the total duration of the observation run.

An inspection of the spectral window function helps to identify which peaks in the periodogram may be alias.

In the top panel of Fig. 3 we plot an example of the spectral window function of our data. Due to the sampling interval of about 1 day imposed by the rotation of the Earth and the fixed longitude of the observation site, the window function has major peaks at $f = \pm n$ cd^{-1} (n integer), together with smaller sidelobes in the range $f = 1 \pm 0.1$ cd^{-1} around the major peak.

In the middle panel of Fig. 3 we plot the effects of the spectral window function on an example strictly periodic signal of $f = 0.2$ cd^{-1} with the same data sampling as the real data. Apart from the power peak corresponding to the true periodic signal at f = 0.2 cd^{-1}, a number of alias peaks appear as consequence of the convolution between the power spectrum and the window function. All these alias periods are beat periods (B) between the star's rotation period (P) and the data sampling and they obey to the relation

$$\frac{1}{B} = \frac{1}{P} \pm n \quad (n = 1, 2, 3, ...) \tag{1}$$

A method to check whether peaks at short periods are beat periods is to perform a prewhitening of the data time series by fitting and removing a sinusoid with the star's rotation period from the data.

In the bottom left panel of Fig. 3 we plot the case of star 1710 whose periodogram shows four peaks with confidence level larger than 99%. Assuming that the highest peak at about f=0.09 cd^{-1} indicates the star's rotation frequency, we see on the bottom right panel of Fig. 3 that, after removing the primary frequency from the data time series and recomputing the periodogram, actually all the other peaks disappear, confirming they are actually beat frequencies.

3.4. Uncertainty with the rotation periods

In order to compute the error associated with the periods we followed the method used by Lamm et al. (2004) where the uncertainty can be written as

$$\Delta P = \frac{\delta\nu P^2}{2} \tag{2}$$

$\delta\nu$ is the finite frequency resolution of the power spectrum and is equal to the full width at half maximum of the main peak of the window function w(ν). If the time sampling is not too non-uniform, which is the case related to our observations, then $\delta\nu \simeq 1/T$, where T is the total time span of the observations. From Eq. (2) it is clear that the uncertainty not only depends on the frequency resolution (total time span) but is also proportional to the square of the period. We computed the error on the period following also the prescription suggested by the Horne & Baliunas (1986), which is based on the formulation given by Kovacs (1981). The uncertainty computed according to Eq. (2) was found to be factor 5-10 larger than by the technique of Horne & Baliunas (1986). In this paper we report the error computed with Eq. (2). Hence, it can be considered as an upper limit, and the precision in the period could be better than that we quote in this paper.

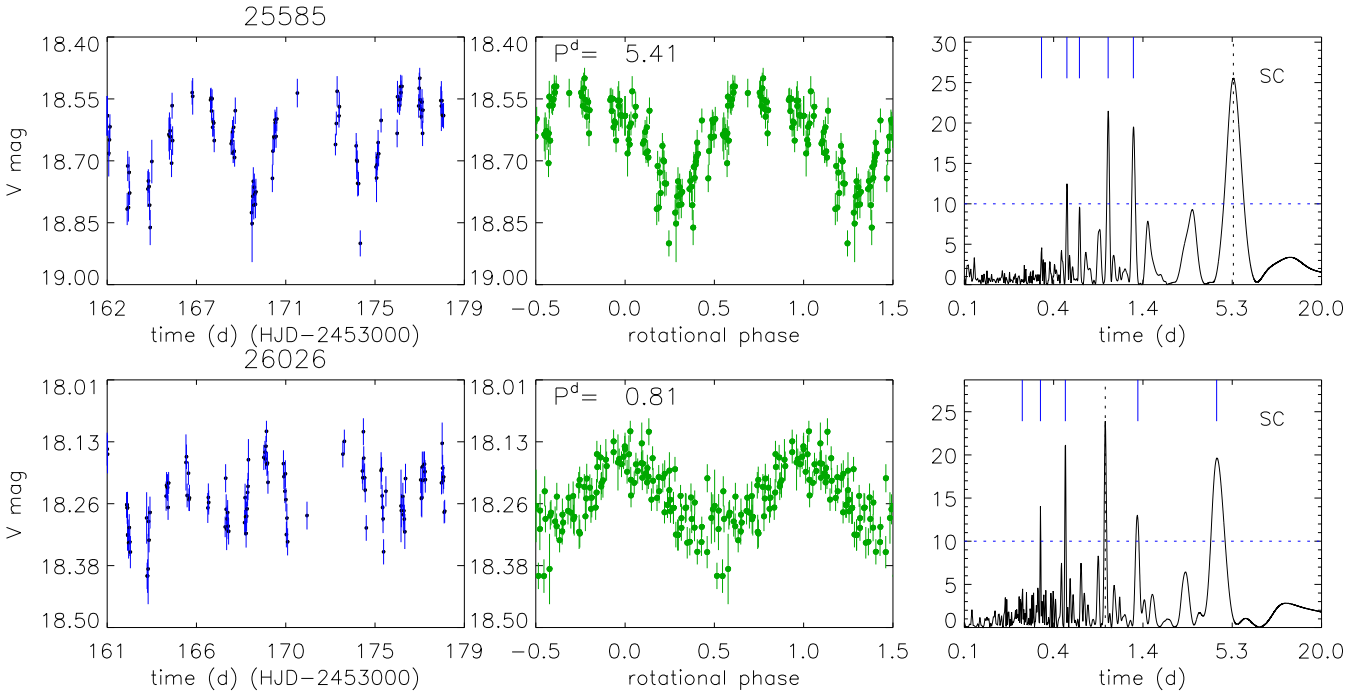

Fig. 4 *From left to right panel:* V-band data time series with uncertainties; folded light curves with phases computed by using the derived period; Scargle normalized periodogram. The vertical dashed line indicates the major peak related to the rotation period, whereas the solid top bars indicates its beat periods.The horizontal dotted line indicates the 99% confidence level.

4. Results

Our period search allowed us to detect 75 new periodic variables in the $22.2' \times 22.2'$ FoV centered in M11. The results are summarized in Table 1 where we list the following information: internal Identification Number (ID); Webda identification number; coordinates (J2000); periodicity (P) and its uncertainty (ΔP); normalised peak power (P_N); average V magnitude (<V>); dereddened $(B-V)_0$ color; photometric accuracy (σ_{acc}); light curve amplitude (ΔV). The latter is computed by making the difference between the median values of the upper and lower 15% light curve normal points (see, e.g., Herbst et al. 2002). That prevents overestimation of the amplitude due to possible residual outliers. We list a note about the membership probability to the cluster, as will be discussed in the next section: 'a' is for high-probability members; 'b' for lower-probability members; 'n' for non-members. Finally, we indicate with a flag 'y' the eclipsing binary systems as classified on the basis of the shape of their light curve. In Fig. 4 we plot, as an example, the results of period search for the stars 25585 and 26026. From left to right panels we plot the V-band magnitude vs. time with overplotted the uncertainties; the phased light curve, which is folded by using the derived period; the Scargle periodogram, where the major power peak related to the observed periodicity is marked by a vertical dotted line, beat periods by solid lines, and the 99% confidence level by dotted horizontal line.

The complete set of 75 light curves, together with Scargle periodograms, are plotted in the online Figs. **??-??**.

5. Discussion

Our major aim is to determine the rotation period distribution and the activity level of the late-type members of M11. Therefore, we have first to identify the cluster members among the 75 newly discovered periodic variables, and subsequently to select only the late-type members whose discovered periodicity is likely related to stellar rotation. We will exclude evident eclipsing binaries from the final sample of periodic late-type members. In fact, due to tidal synchronization, the rotational evolution of the components of close binary systems significantly differs from the evolution history of single stars, on which we are focussed.

5.1. Candidate member selection

M11 has a very rich stellar background and it is a very difficult task to identify the cluster members. The proper motion studies carried out by McNamara et al. (1977), Su et al. (1998), and Dias et al. (2006) provide information only on the bright (V< 16 mag) members. The radial velocity survey carried out by Mathieu et al. (1986) is also limited to a handful of stars. Our proposed periodic variables have information neither on proper motion nor on radial velocity. So we have left no option other than using the following two criteria to identify cluster members: *i)* the photometric membership, that is the distance of any star from the theoretical isochrone in the color-magnitude diagram (see, e.g., Irwin 2006, 2008); *ii)* the spatial distance from the cluster center.

In Fig. 5 we plot the color-magnitude V vs. B−V (left panel) and V vs. V−I (right panel) diagrams of all stars (small dots) detected in our FoV. The B−V colors are ours, whereas the V−I colors are taken from Sung et al.

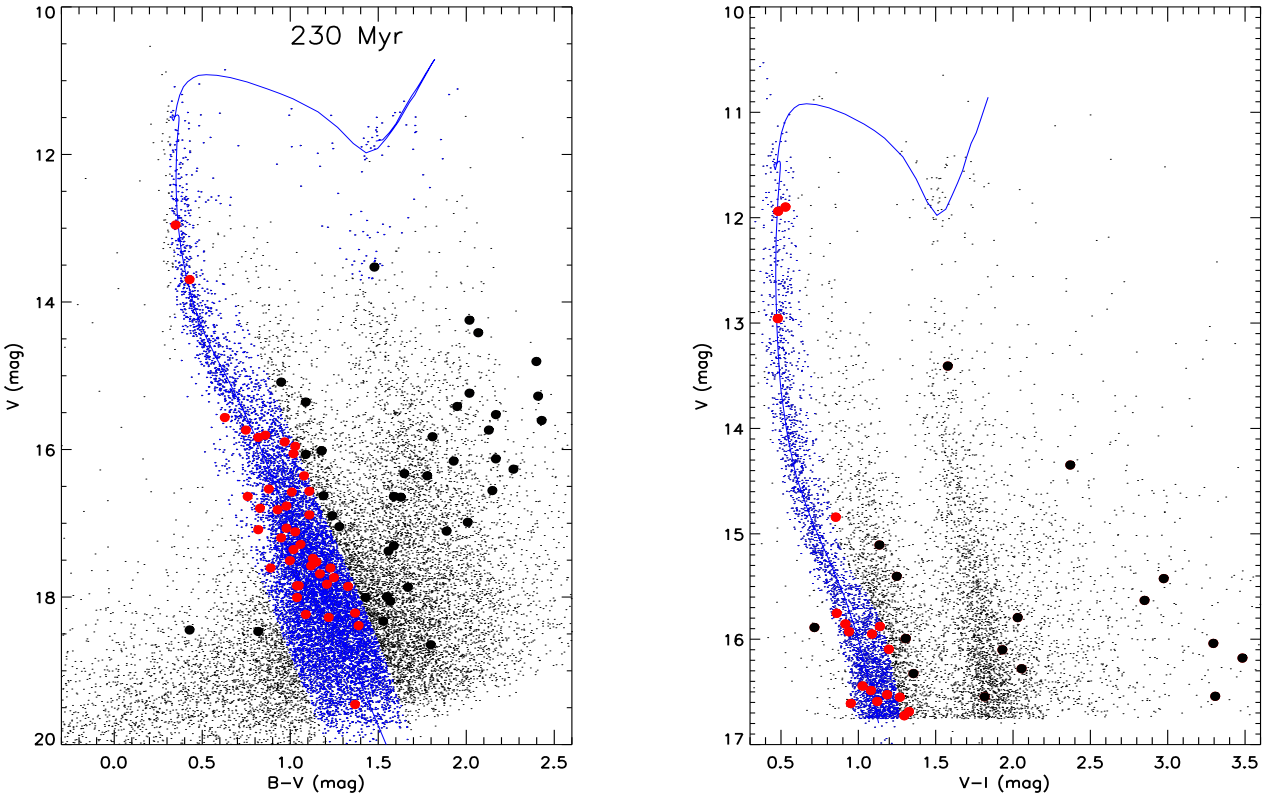

Fig. 5 *Left panel:* V vs . B−V diagram of the stars (dots) detected in the 22.2′×22.2′ field of M 11. Photometric candidate members are plotted with blue small bullets, newly-discovered periodic candidate members are plotted with red large and black bullets. The solid line represents the isochrone corresponding to an age of log t=8.35, E(B−V) = 0.428 mag, (m−M)=12.69 mag (Sung et al. 1999). *Right panel*:same as left panel but with V−I colors from Sung et al. (1999). Note that neither V nor V−I values are available for stars fainter than ∼ 16.7.

(1999) and available only for stars brighter than V≃ 16.7. We overplot the color-reddened 230-Myr isochrone derived from Girardi et al. (2000), and corresponding to the cluster parameters taken from Sung et al. (1999).

In the first criterion, we assign two probability levels on the basis of the distance from the isochrone: '1a' to stars with distance smaller than ±(1.4+σ) mag (blue small dots in Fig. 5), '1b' to stars with distance larger than ±(1.4+σ) mag (black small dots) in the case of V vs. B−V diagram. Similarly, we assign '2a' and '2b' in the case of the V vs. V−I diagram. Red bullets represent the proposed periodic variables with probability membership '1a' (left) and '2a' (right), whereas black bullets represent the proposed periodic variables with probability membership '1b' and '2b', respectively. The quantity σ takes into account the increasing photometric uncertainty towards fainter stars.

In the second criterion, we assign two probability levels on the basis of the projected angular distance from the cluster center and the relative density distribution shown in Fig. 6: '3a' to stars with distance smaller than 10′, '3b' to stars with distance larger than 10′.

As a final result, we assign a high-probability flag 'a' to stars having contemporarily '1a', '2a', and '3a'; a lower-probability flag 'b' to stars having '1a', '3a' and no measured V−I color. All the remaining stars are classified to be non members 'n' and are excluded from the analysis of the cluster rotation period distribution. The probability flags are listed in Table 1.

Our final sample of newly discovered variables consists of: 9 high-probability members (4 early-type stars with $(B-V)_0<$ 0.5, 5 late-type stars with $(B-V)_0\geq$ 0.5); 29 lower-probability members (2 early-type, 25 late-type, 2 eclipsing binaries); 37 non members which will not considered in the following analysis. In Fig. 7 we plot the 2 newly discovered eclipsing binaries cluster members.

5.2. Rotation period distribution

As anticipated, our attention is focussed on the late-type members of M 11. In fact, the detected periodicity of these late-type stars most likely represents the stellar rotation period. The variability observed over time scales from several hours to days arises from non-uniformly distributed, cool-spotted regions on the stellar photosphere, which are carried in and out of view by the star's rotation. We excluded from our analysis all periodic variables bluer than

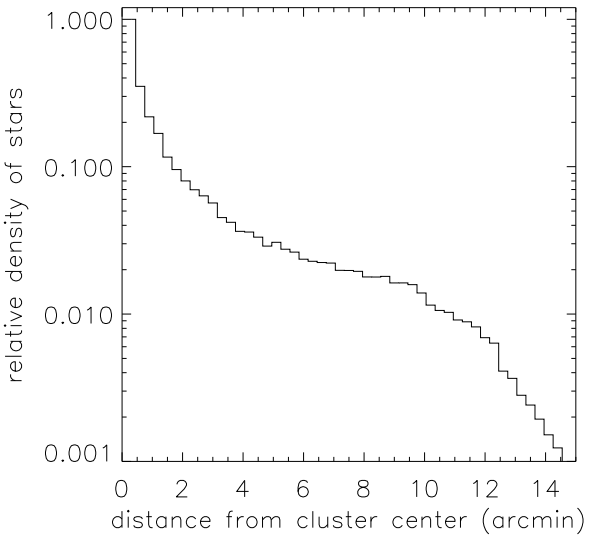

Fig. 6 Relative density of stars in the M11 FoV with respect to the cluster center.

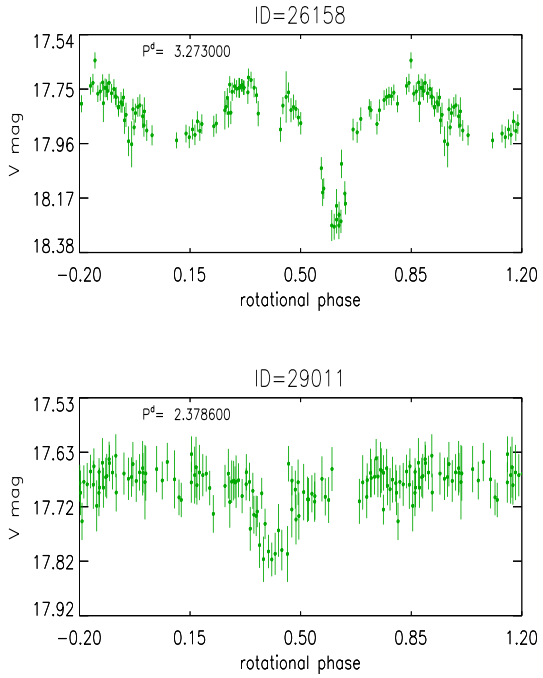

Fig. 7 Eclipsing binaries newly discovered among periodic members of M11 .

$(B-V)_0$=0.5, whose periodic variability is likely related to pulsations. We excluded also the already known (see Koo et al. 2007) as well as the newly discovered W UMa-type and detached eclipsing binaries, their angular momentum evolution being altered by tidal synchronization between stellar components.

All periodic members discovered by us have $(B-V)_0$<0.9, which roughly corresponds to main sequence stars of spectral type earlier than K2/3 and mass $M/M_\odot \gtrsim 0.8$. Therefore, our analysis has provided for the first time the rotation period distribution of the G-type and early-K members of M11. The absence of periodic middle-K or later-type stars must be ascribed to the lower photometric accuracy, which becomes comparable to or larger than the periodic variability amplitude due to starspots for the fainter stars.

In Fig. 8 we plot the rotation period distribution of late-type (bona-fide) single stars vs. the $(B-V)_0$ color. Different symbols are used to plot stars with different levels of membership probability to the cluster, according to the criteria outlined in the previous Section. Specifically, 5 stars are found to be high-probability members ('a') and plotted with filled bullets; 16 stars have a lower membership probability ('b') and are plotted with open circles. Here we like to remind that such lower probability level of membership arises from unavailability of V−I measurements (see right panel of Fig. 5). In the following analysis we consider all together, although plotted with different symbols, both stars with 'a' and 'b' membership probability.

A cluster of slightly younger age (about 200 Myr) and with known rotational properties is M34 (Irwin et al. 2006). The survey of Irwin et al. (2006) allowed to determine the rotation period distribution of the lower-mass K-M stars. In Fig. 8 we plot with partially filled-in bullets the 16 periodic variables of M34 with spectral type earlier than K2. The original $(V-I)_0$ colors in Irwin et al. have been transformed into $(B-V)_0$ colors by using standard stars color-color relations (Cox 2000). These additional data allow us to get a more numerous sample of periodic stars and, consequently, to derive a reliable rotation period distribution of G0-K2 stars at an age of about 200-230 Myr.

As observed in other young open clusters, also the M11 members are found to distribute between two different rotation regimes. There is a fraction of stars whose rotation period is larger than about 1-2 days. Their distribution displays an upper envelope which increases with increasing B−V color. These stars belong to the so called 'interface sequence', according to the classification scheme of Barnes (Barnes 2003). These stars have experienced the effects of rotation braking by stellar magnetized winds, and are expected to continue slowing down to reach, by an age of about 500-600 Myr, a one-to one dependence between rotation period and color (see, e.g., Collier Cameron et al. 2009). A second fraction of stars with period smaller than 1-2 days belongs to the so called 'convective sequence'. They have not experienced yet significant spin down and are progressively moving towards the interface sequence of slow rotators. Bluer stars in this sequence leave first and the B−V color at which the sequence begins varies with the cluster age. The solid line is the theoretical curve, computed by using Eq. (1) of Barnes (2003) - $P=\sqrt{(t)}$ f(B−V) where f(B−V) represents the color dependence of the data -. It represents the expected upper envelope of the rotation period distribution at a nominal age of $\sim$ 230 Myr, assuming a rotation rate decay according to the Skumanich law (Skumanich 1972). We refer the reader to Barnes (2003) for a detailed description of both sequences. The agreement between the observed interface

sequence and its expected distribution is quite good and gives support to the estimated cluster age.

From our analysis we find that the G-type members of M11 have a median rotation period of P=4.8 days. This is the first determination of median rotation period of G-type stars at an age of 230 Myr, which is the only available value in the age range from 150 Myr (M35) to 550 Myr (M37).

5.3. Angular momentum evolution

The variation vs. time of the median rotation period of cluster members is the quantity generally used to detect and investigate the rotational evolution of low-mass stars.

In the right panel of Fig. 8, we compare the rotation period distribution of M11 with the distributions of the younger open cluster M35 (150 Myr; Meibom et al. 2009) and of the older open cluster M37 (550 Myr; Hartman et al. 2009; Messina et al. 2008a). Focussing our attention on the G-type slow rotating stars of these clusters, that is on stars in the interface sequence and in the $0.55 < (B-V)_0 < 0.9$ colour range, we find that the median rotation periods are P_{M35}=4.4d, P_{M11}=4.8d, P_{M37}=6.8d. This is the major result of our analysis: we have determined the median rotation period of G stars at an age of 230 Myr, at which to date no information on rotational properties was available. Moreover, the comparison with the median period of two other clusters shows that the value we found is consistent with the expected rotation slow down with age.
We plot the age-parameterized family of theoretical curves corresponding to nominal ages of $\sim$ 150 Myr (black dotted line) $\sim$ 230 Myr (red solid line), and $\sim$ 550 (blue dashed line). The younger gyro-isochrones (150 and 230 Myr) appear to fit the observed distribution upper envelopes better than the older gyro-isochrone at 550 Myr. However, this discrepancy depends on the parametric curve rather than on the age of M37, which is quite well established (see Hartman et al. 2009). Two important results arise from comparing data with isochrones. First, the agreements shows the validity of the Skumamnich rotation rate decay, that is a dependence of rotation on square root of time. Second, the Barnes parameterization very well reproduces the observed rotation period distribution at an age of about 230 Myr.

Now we turn our analysis to the fast rotators. In this case we note some sort of discrepancy with respect to the younger cluster M35. In fact, in M35 the convective sequence begins approximately at $(B-V)_0$=0.8. We expect in older clusters such sequence to begin at redder colors. On the contrary, we note in both M34 and M11 a number of fast rotating stars bluer than$(B-V)_0 < 0.8$. Actually, this discrepancy may be explained without need of contradicting the rotation evolutionary sequence described above. Firstly, we see that these unexpected blue fast rotators have lower membership probability. As discussed by Sung et al. (1999) the cluster is at low galactic latitude ($\sim -3°$), near the Scutum star cloud and the Sagittarius-Carina arm, resulting in very large contamination of the cluster color-magnitude diagram from the relatively young (and, therefore, fast rotating) field population. Therefore, these blue fast rotators may just be interlopers. Alternatively, some of these fast rotators may be cluster members, but they may belong to close binaries of BY Dra, RS CVn, W UMa or FK Com types, which are not identified as such variables, yet, and are rapidly rotating due to tidal interaction and synchronisation. Indeed, all the already known and newly discovered binary stars with $(B-V)_0 > 0.5$ and with high-probability membership, if plotted in Fig. 8, would all populate the convective sequence. A third possibility may be the false detections of the periods. For example, the presence of two activity centers in the stellar photosphere at the epochs of observations, about 180° away in longitude from each other, can produce a light modulation with half of the true rotation period. In these cases, consecutive observation seasons are needed to detect the true rotation period (Parihar et al. 2009).

5.4. Photospheric activity

The photometric variability we observed in the proposed late-type periodic members of M11 arises from the presence of cool photospheric spots whose visibility is modulated by the stellar rotation. The total amount of cool spots is related to surface magnetic fields, whose filling factor depends on the rotation rate and on the depth of the convection zone (or mass). The amplitude of the observed variability, specifically the peak-to-peak light curve amplitude, is suitable to trace the dependence of the magnetic field filling factor on rotation and mass. In Fig. 9 we plot the amplitude of the V-band light curve of the M11 late-type periodic members together with the M34 members. The symbols have same meaning than in Fig. 8. We see that the upper envelope of the light curve amplitude decreases with increasing rotation period. This is consistent with the expected dependence on rotation rate of the efficiency of magnetic filed generation and intensification by an $\alpha\Omega$ dynamo. The solid line represents the fit to the upper envelope of the light curve amplitude distribution of slow rotating Pleiades G stars (110 Myr) taken from Messina et al. (2001, 2003). With the data at our disposal, we do not see any significant difference between the 110-Myr and the 230-Myr distribution upper envelopes. Our sample of only G stars does not allow us to say anything about the mass dependence of the amplitude-rotation relation.
As discussed in Paper I, there is some marginal (yet) evidence of the existence of some other age-dependent quantity, in addition to mass and rotation, that controls the level of (photospheric at least) activity, and makes older stars less active than younger stars (see also Messina et al. 2009). A similar suspect was already raised by Messina et al. (2001), who found evidence that, for a fixed mass and rotation period, the level of starspot activity increases (or alternatively the gross surface distribution of spots changes) from the zero-age main sequence up to the Pleiades age ($\sim$120 Myr) and then it decreases with age. With the data of M11 G stars in our hand we can state that up the the M11 age the level of activity remains at highest levels. On the contrary, the K-type stars at an age of 200 Myr already show a significantly decreased activity with respect to the younger K-type Pleiades stars, as shown in Fig. 16 of the paper by Irwin et al. (2006).

It is interesting to note that, when we select the final sample of periodic variables to determine the rotation period distribution, the existence of a rotation-activity relation provides an independent tool to identify either possible binary systems or erroneous period determination. In fact, due to eclipse minima and enhanced rotation with re-

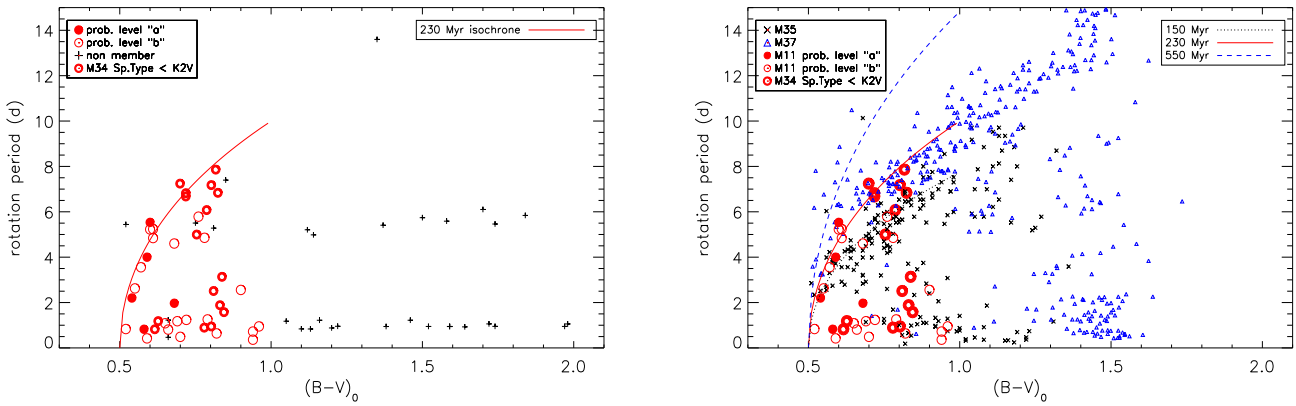

Fig. 8 *Left panel*: Rotation period vs. $(B-V)_0$ colour for the members of M11. Different symbols are used to represents high- and low membership probability. The periods of the M34 members with spectral type earlier than K2/3 are also plotted. The solid curve represents the gyro-isochrone at a nominal age of 230 Myr. *Right panel*: same as left panel, but with overplotted the rotation period distribution of M37 (triangles) and M35 (asterisks). The family of age-parameterised curves from gyrochronology corresponding to ages of 150, 230 and 550 Myr is overplotted.

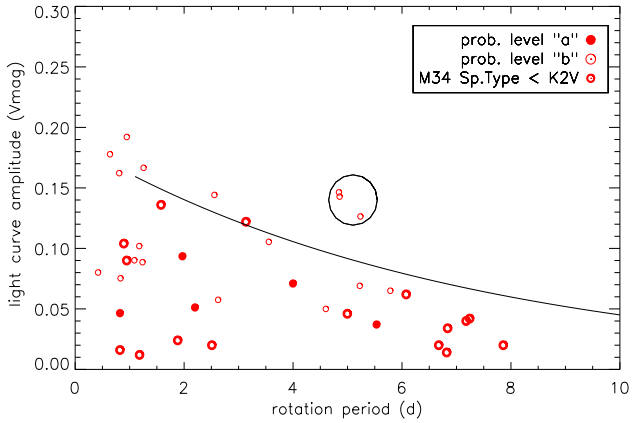

Fig. 9 V-band light curve amplitude (ΔV) vs. rotation period for the same stars plotted in the left panel of Fig. 8. The solid line represents the upper envelope of the ΔV vs. rotation period distribution of dwarf G stars from Messina et al. (2003), whereas the circled three stars above such boundary are suspected binary stars.

spect to single stars, close binaries show light curve amplitudes much larger than observed in single stars. Similarly, an incorrect period determination, specifically an incorrect value larger than the true rotation period (e.g. its beat period), produces an outlier in the rotation-activity distribution. Such outliers allow us to identify, or at least to defer for additional study, stars which may contaminate the final sample. In our case, the stars 10861, 18776 and 22541 (which are circled in Fig. 9) show a light curve amplitude larger than ever observed in stars of similar mass and rotation period. Follow-up observations may reveal that the adopted period is actually the (long) beat period. Similarly, this method can allowus to identify, and consequently exclude from the final sample, W-UMa close binaries whose light curve amplitudes clearly deviate from the distribution upper envelope and whose light curve shape are much scattered to identify its W UMa nature.

6. Conclusions

We have analysed V-band magnitude time series of the young 230-Myr open cluster M11 collected in 2004 at the LOAO observatory. Our analysis has allowed us to derive the following results:

- We have discovered 75 new periodic variables in a 22.2′x 22.2′ FoV centered in M11. Considering that 64 periodic variables were known from earlier studies, the total number of known periodic variable in this FoV is 139.
- 2 newly discovered periodic variable members are likely eclipsing binary systems. The discovery of such systems, whose absolute physical parameters can be determined with spectroscopic and multiband photometric follow-up studies, is relevant to better determine the distance to the cluster as well as to the understanding of the dynamical evolution of binary systems at intermediate age.
- Out of 75 new periodic variables, we have found that 30 stars are likely single late-type periodic cluster members. Such stars have colors in the range $0.5<(B-V)_0<0.9$, which corresponds to main sequence spectral type earlier than K2 and stellar mass larger than 0.8 $M_\odot$.
- By adding to our data 16 G-type periodic variables belonging to the almost coeval cluster M34 and taken from the literature, we have determined from a sample of 46 stars the median rotation period P=4.8d of the G stars at an age of about 200-230 Myr for the first time. In fact, the rotational properties of G stars in the age range 150-550 Myr were unknown before the present study.
- The median period we determined is longer than the median period P=4.4d of G stars in the younger cluster M35+M34 and shorter than the median period P=6.8d of G stars in the older cluster M37. This result is in good agreement with the expected scenario of rotation spin down with age according to the Skumanich rotation decay law.
- The distribution of the light curve amplitude of G-type members of M11 is found to decrease with increasing rotation period. This activity-rotation relation is found

either in other open clusters or in field stars and supports the expected operation of an $\alpha\Omega$ dynamo whose efficiency is related to both rotation and convection zone depth. The average level of acitvity of these 230Myr old stars is found to be comparable to the activity level of the younger Pleiades stars.

Acknowledgements. This work was supported by the Italian Ministero dell'Università, Istruzione e Ricerca (MIUR) and the National Institute for Astrophysics (INAF). The extensive use of the SIMBAD and ADS databases operated by the CDS center, Strasbourg, France, is gratefully acknowledged. This research has made use of the WEBDA database, operated at the Institute for Astronomy of the University of Vienna. We thank the Referee for very useful comments and suggestions.

References

Bailer-Jones, C. A. L., & Mundt, R. 2001, A&A, 367, 218
Barnes, S. 2003, ApJ, 586, 464
Barnes, S. 2007, ApJ, 669, 1167
Bouvier, J., Forestini, M., & Allain, S. 1997, A&A, 326, 1023
Cox, A.N. 2000, in Allen's Astrophysical Quantities, 4th Edition, (Springer, AIP Press)
Girardi, L., Bressan, A., Bertelli, G., & Chiosi, C. 2000, A&AS, 141,371
Gonzalez, G., & Wallerstein, G. 2000, PASP, 112, 1081
Guinan, E. F., McCook, G. P., DeWarf, L. E., et al. 2003, Bulletin of the American Astronomical Society, 35, 766
Dias, W. S., Assafin, M., Flório, V., Alessi, B. S., & Lbero, V. 2006, A&A, 446, 949
Hargis, J.R., Sandquist, E.L., & Bradsteert, D.H. 2005, AJ, 130, 2824
Hartman, J.D., Gaudi, B.S., Pinsonneault, M.H., et al. 2009, ApJ, 691, 342
Herbst, W. & Wittenmyer, R. 1996, BAAS, 28, 1338
Herbst, W., Bailer-Jones, C. A. L., Mundt, R., Meisenheimer, K., & Wackermann, R., 2002, A&A, 396, 513
Herbst, W., & Mundt, R. 2005, ApJ, 633, 967
Hodgkin, S.T., Irwin, J.M., Aigrain, S., et al. 2006, AN, 327, 9
Holzwarth, V., & Jardine, M. 2007, A&A, 463, 11
Horne, J. H. & Baliunas, S. L. 1986, ApJ, 302, 757
Irwin, J., Aigrain, S., Hodgkin, S., et al. 2006, MNRAS, 370, 954
Irwin, J., Hodgkin, S., Aigrain, S., et al. 2007, MNRAS, 377, 741
Irwin, J., Hodgkin, S., Aigrain, S., et al. 2008, MNRAS, 383, 1588
Ivanova, N., & Taam, R. E. 2003, ApJ, 599, 516
Kang, Y.B., Kim, S.-L., Rey, S.-C., et al, 2007, PASP, 119, 239
Kawaler, S.D., 1988, ApJ, 333, 236
Kim, S.-L., Chun, M.-Y., Park, B.-G. et al. 2001, A&A 371,571
Koo, J,-R., Kim, S.-L., Rey, S.-C. et al. 2007, PASP, 119, 1233
Kovacs G., 1981, Ap&SS, 78, 175
Krishnamurthi, A., Pinsonneault, M. H., Barnes, S., & Sofia, S. 1997, ApJ, 480, 303
Lamm M. H., Bailer-Jones C. A. L., Mundt R., Herbst W., Scholz A., 2004, A&A, 417, 557
MacGregor, K. B., & Brenner, M. 1991, ApJ, 376, 204
Martn, E.L., Dahm, S., & Pavlenko, Y. 2001, ASP Conference Series Vol. 245. Ed. Ted von Hippel, Chris Simpson, and Nadine Manset. San Francisco, p.349
Mathieu R. D., & Latham D. W., 1986, AJ, 92, 1364
McNamara, B.J., Pratt, N.M., & Sanders, W.L. 1977, A&AS, 27, 117
Meibom S., Mathieu R. D., & Stassun K. G., 2009, ApJ, 695, 679
Messina, S., Rodonò, M., & Guinan, E. F. 2001, A&A, 366, 215
Messina, S., Pizzolato, N., Guinan, E. F., & Rodonó, M. 2003, A&A 410, 671
Messina, S., 2007, Mem. Soc. Astron. It., 78, 628
Messina, S., Distefano, E., Parihar, P., et al. 2008a, A&A, 483, 253
Messina, S., 2008b, A&A, 480, 495
Messina, S., Desidera, S., Turatto, M., Lanzafame, A.C., & Guinan, E.F. 2009, submitted to A&A
Meynet,G., Mermilliod, J-.C., Maeder, A. 1993, A&AS, 98, 477
Parihar, P., Messina, S., Distefano, E., Shantikumar, N. S., & Medhi, B. J. 2009, MNRAS, 400, 603
Press, W.H., Teukolsky, S.A., Vetterling, W.T., & Flannery, B.P. 1992, in Numerical recipes in FORTRAN, Cambridge: University Press, 1992, 2nd ed.
Radick, R.R., Lockwood, G.W., Skiff, B.A., & Thompson, D.T. 1995, ApJ, 452, 332
Rebull, L.M., Wolff, S.C., & Strom, S.E. 2004, AJ, 127, 1029
Roberts, D. H., Lehar, J., & Dreher, J. W. 1987, AJ, 93, 978
Roze, M.B. & Hintz E.G., 2007, AJ, 134, 2067
Scargle, J.D. 1982, ApJ, 263, 835
Sills, A., Pinsonneault, M. H., & Terndrup, D. M. 2000, ApJ, 534, 335
Skumanich, A. 1972, ApJ, 171, 565
Stassun, K.G., Mathieu, R.D., Mazeh, T., & Vrba, F. 1999, AJ, 117, 2941
Su C.-G., Zhao J.-L., & Tian K.-P., 1998, A&AS, 128, 255
Sung,H., Bessel, M.S., Lee, H.-W., Kang, Y-H-. & Lee, S.-W., 1999, MNRAS, 310, 982
von Braun, K., Lee, B. L., Seager, S., et al. 2005, PASP, 117, 141

Table 1. Summary of period search: Star's internal identification number (ID); Webda number; Right Ascension and Declination; Period (P) and and its uncertainty (ΔP); Normalised peak power (P_N); Average V magnitude (<V>); Dereddened B−V color; Photometric accuracy (σ_{acc}), Light curve amplitude (ΔV); Membership probability; note on binarity based on light curve shape.

ID	ID Webda	RA (hh:mm:ss)	DEC (dd:mm:ss)	P±ΔP (d)	P_N	<V> (mag)	$(B-V)_0$ (mag)	σ_{acc} (mag)	ΔV (mag)	Mem prob.	Binary
185	241	18:51:36.204	-06:16:40.24	0.94 ± 0.01	15.98	13.91	1.59	0.0094	0.0602	n	
195	253	18:51:35.597	-06:09:11.90	0.466 ± 0.003	16.73	14.74	0.66	0.0111	0.0483	n	
227	290	18:51:33.843	-06:20:27.27	0.94 ± 0.01	21.06	14.09	1.52	0.0073	0.1116	n	
414	493	18:51:22.576	-06:21:51.37	0.249 ± 0.001	15.08	14.24	0.20	0.0793	0.1723	b	
444	525	18:51:20.999	-06:14:01.33	0.249 ± 0.001	15.93	14.48	0.43	0.0096	0.0762	b	
530	617	18:51:17.083	-06:13:39.61	0.95 ± 0.01	16.19	13.48	1.97	0.0093	0.0980	n	
957	1075	18:51:04.289	-06:25:05.07	0.92 ± 0.01	27.22	13.09	1.64	0.0090	0.0817	n	
1292	1433	18:50:55.568	-06:23:36.96	0.95 ± 0.01	16.26	11.63	-0.08	0.0080	0.0444	a	
1509	1660	18:50:45.538	-06:12:54.69	2.19 ± 0.08	22.77	14.57	0.54	0.0114	0.0512	a	
1606	1763	18:50:40.704	-06:14:44.25	1.23 ± 0.02	16.58	14.03	0.66	0.0076	0.0383	n	
1647	1805	18:50:38.869	-06:13:12.26	0.94 ± 0.01	19.10	12.92	1.59	0.0074	0.0742	n	
1663	1822	18:50:38.184	-06:13:51.35	1.18 ± 0.02	16.42	12.20	1.05	0.0091	0.0647	n	
1719	1880	18:50:35.151	-06:12:50.15	5.4 ± 0.4	17.45	13.76	0.52	0.0103	0.0319	n	
1733	1896	18:50:34.613	-06:25:05.34	20.0 ± 0.7	40.27	14.28	2.00	0.0112	0.1112	n	
2098	...	18:51:00.154	-06:14:49.72	0.434 ± 0.009	28.45	12.37	0.00	0.0212	0.1073	b	
3662	5005	18:50:28.031	-06:10:09.14	0.95 ± 0.01	23.17	14.20	1.74	0.0173	0.0596	n	
3860	5203	18:50:32.581	-06:14:57.60	5.5 ± 0.4	22.06	14.80	1.74	0.0099	0.0729	n	
3867	5210	18:50:32.763	-06:20:04.30	1.05 ± 0.01	32.74	13.95	1.98	0.0272	0.0918	n	
3987	5330	18:50:35.453	-06:09:19.30	1.06 ± 0.01	22.89	15.23	1.72	0.0197	0.0911	n	
4061	5404	18:50:37.144	-06:10:04.81	0.822 ± 0.003	16.67	15.25	0.58	0.0167	0.0465	a	
4122	5465	18:50:38.537	-06:14:37.02	5.5 ± 0.4	18.98	14.69	0.75	0.0111	0.0437	n	
4197	5540	18:50:40.578	-06:22:35.36	1.97 ± 0.05	38.20	15.24	0.68	0.0202	0.0935	a	
4244	5587	18:50:41.695	-06:12:57.87	0.82 ± 0.01	25.61	14.51	0.39	0.0157	0.0443	a	
4291	5634	18:50:42.840	-06:15:42.38	0.95 ± 0.01	23.54	15.00	1.22	0.0141	0.1600	n	
4341	5684	18:50:43.663	-06:16:53.12	1.08 ± 0.01	24.64	15.03	0.65	0.0122	0.0902	b	
4370	5713	18:50:44.146	-06:12:07.95	1.24 ± 0.02	19.69	15.31	0.33	0.0362	0.0916	a	
4374	5717	18:50:44.235	-06:14:34.73	1.25 ± 0.02	21.36	15.21	0.45	0.0346	0.0743	a	
4547	5890	18:50:47.746	-06:21:29.32	1.21 ± 0.02	15.13	15.31	1.16	0.0132	0.0572	n	
4549	5892	18:50:47.769	-06:10:33.49	5.5 ± 0.4	24.59	14.63	0.60	0.0201	0.0371	a	
4556	5899	18:50:47.853	-06:11:06.86	14 ± 3	48.12	15.03	1.35	0.0159	0.2109	n	
5367	6710	18:51:03.950	-06:23:03.13	6.1 ± 0.5	17.73	14.41	1.70	0.0074	0.0652	n	
5477	6820	18:51:06.144	-06:10:08.84	5.7 ± 0.5	27.66	14.83	1.50	0.0131	0.1068	n	
6370	7713	18:51:22.449	-06:11:15.40	5.7 ± 0.5	25.76	15.30	0.76	0.0173	0.0650	b	
6428	7771	18:51:23.829	-06:25:36.70	4.0 ± 0.2	30.36	14.73	0.59	0.0099	0.0710	a	
6440	7783	18:51:24.012	-06:13:20.38	1.888 ± 0.003	39.03	14.50	1.38	0.0090	0.0816	n	
6756	8099	18:51:31.434	-06:13:53.09	5.8 ± 0.5	17.80	14.94	1.84	0.0154	0.0968	n	
8594	10095	18:51:10.248	-06:06:01.43	1.244 ± 0.005	15.68	17.14	0.39	0.0609	0.1338	n	
9517	10696	18:51:41.247	-06:07:18.46	0.88 ± 0.01	20.16	15.32	1.20	0.0129	0.1028	n	
10052	11078	18:51:19.119	-06:07:55.82	7.4 ± 0.8	15.01	15.72	0.85	0.0197	0.0591	n	
10161	11155	18:50:41.777	-06:08:03.78	21.05 ± 0.01	41.28	16.54	1.24	0.0552	0.3606	n	
10851	11629	18:50:55.996	-06:09:02.21	4.6 ± 0.3	17.85	15.56	0.68	0.0146	0.0500	b	
10861	11637	18:50:54.708	-06:09:02.51	5.2 ± 0.4	16.05	16.68	0.61	0.0568	0.1264	b	
12485	12774	18:50:54.307	-06:11:09.85	5.2 ± 0.4	30.33	15.79	0.60	0.0150	0.0691	b	
12646	12890	18:50:52.443	-06:11:23.12	2.6 ± 0.1	23.89	15.74	0.55	0.0150	0.0575	b	
13073	13214	18:51:12.981	-06:11:58.35	1.22 ± 0.02	15.74	15.78	1.46	0.0202	0.0809	n	
13511	13536	18:51:44.895	-06:12:34.27	0.327 ± 0.001	33.78	16.28	0.46	0.0419	0.2369	b	
13540	13556	18:50:56.759	-06:12:35.98	5.3 ± 0.4	15.95	15.57	0.81	0.0237	0.0752	n	
13951	13849	18:51:37.563	-06:13:11.24	1.25 ± 0.02	18.47	16.95	0.79	0.0718	0.1666	b	
14095	13950	18:50:48.687	-06:13:24.10	3.5 ± 0.1	18.25	16.18	0.57	0.0339	0.1054	b	
14450	14207	18:50:27.796	-06:13:55.76	2.5 ± 0.1	24.80	16.53	0.90	0.0467	0.1442	b	
15291	14792	18:51:18.248	-06:15:18.63	0.83 ± 0.01	15.54	16.05	1.13	0.0312	0.0781	n	
15633	15020	18:50:43.468	-06:15:50.88	5.6 ± 0.4	18.04	15.66	1.58	0.0172	0.0428	n	

Table 1 (cont'd)

ID	ID Webda	RA (hh:mm:ss)	DEC (dd:mm:ss)	P±ΔP (d)	P_N	<V> (mag)	$(B-V)_0$ (mag)	σ_{acc} (mag)	ΔV (mag)	Mem prob.	Binary
17415	16297	18:51:26.378	-06:18:44.88	0.420 ± 0.002	18.54	16.03	0.59	0.0217	0.0801	b	
17546	16397	18:50:39.657	-06:18:53.31	0.83 ± 0.01	16.12	17.00	1.10	0.0989	0.3246	n	
17649	16470	18:50:30.580	-06:19:03.98	0.362 ± 0.002	22.86	16.89	0.94	0.2341	0.3098	b	
17730	16528	18:50:41.216	-06:19:05.59	5.2 ± 0.4	22.95	16.67	1.12	0.0311	0.1987	n	
18776	17281	18:51:10.130	-06:20:29.10	4.8 ± 0.3	18.16	16.52	0.61	0.0364	0.1463	b	
19357	17726	18:50:35.405	-06:21:13.05	1.18 ± 0.02	17.35	16.25	0.69	0.0259	0.1019	b	
19570	17883	18:50:51.008	-06:21:31.20	0.83 ± 0.01	22.48	15.87	0.52	0.0269	0.0753	b	
19844	18088	18:50:41.003	-06:21:53.06	0.2214 ± 0.0007	40.20	15.98	1.16	0.0267	0.6817	n	y
21243	19140	18:50:39.625	-06:23:35.99	0.488 ± 0.003	15.20	16.15	0.70	0.1086	0.3077	b	
22541	20108	18:50:53.732	-06:25:09.70	4.8 ± 0.3	19.88	16.50	0.78	0.0346	0.1428	b	
23809	21055	18:51:17.696	-06:26:45.79	0.95 ± 0.01	27.95	17.06	0.96	0.0380	0.1921	b	
23878	21104	18:50:36.522	-06:26:49.94	1.85 ± 0.01	23.06	16.68	1.00	0.0495	0.3521	n	y
25585	22164	18:50:30.755	-06:19:07.60	5.4 ± 0.4	25.54	17.32	1.37	0.0697	0.2707	n	
26026	22451	18:50:33.299	-06:24:22.86	0.81 ± 0.01	23.91	16.91	0.66	0.0561	0.1622	b	
26072	22483	18:50:29.833	-06:24:46.87	0.720 ± 0.009	16.18	18.13	0.94	0.1793	0.3507	b	
26158	22536	18:50:34.161	-06:25:35.99	3.2884 ± 0.04	25.61	16.52	0.62	0.0839	0.4506	b	y
27360	23360	18:51:01.356	-06:11:07.67	0.396 ± 0.002	23.60	15.76	0.39	0.0296	0.1788	b	
29011	24388	18:51:45.297	-06:21:07.52	2.38 ± 0.09	16.53	16.36	0.74	0.0744	0.1153	b	y
29195	...	18:50:27.943	-06:05:40.81	0.95 ± 0.01	20.24	17.12	0.00	0.0918	0.2132	n	y
30166	25180	18:51:01.500	-06:18:41.95	1.23 ± 0.02	20.62	15.47	0.40	0.0243	0.0715	b	
30525	25503	18:51:29.387	-06:15:22.32	0.639 ± 0.006	32.82	16.41	0.82	0.0357	0.1778	b	
34773	26477	18:50:22.444	-06:13:50.70	1.23 ± 0.4	18.01	16.20	0.72	0.0279	0.0886	b	
35526	26763	18:50:56.030	-06:09:42.59	5.0 ± 0.3	27.36	16.73	1.14	0.0435	0.2130	n	

List of Objects

'M11' on page 1
'M37' on page 1
'M11' on page 1
'M11' on page 1
'M 11' on page 2
'Pleiades' on page 2
'M 11' on page 2
'M 11' on page 3
'M 11' on page 6
'M 11' on page 6
'Pleiades' on page 8
'Pleiades' on page 8
'M11' on page 9
'M37' on page 9
'M35' on page 9